IVYSPRING INTERNATIONAL PUBLISHER

International Journal of Biological Sciences

2019; 15(2): 277-286. doi: 10.7150/ijbs.30348

Research Paper

Icariin Inhibits Endoplasmic Reticulum Stress-induced Neuronal Apoptosis after Spinal Cord Injury through Modulating the PI3K/AKT Signaling Pathway

Haotian Li[1, 2*], Xinran Zhang[3*], Xi Qi[1, 2*], Xu Zhu[1, 2], Liming Cheng[1, 2]✉

1. Department of Spine Surgery, Tongji Hospital, Tongji University School of Medicine, Shanghai 200065, China.
2. Key Laboratory of spine and spinal cord injury repair and regeneration (Tongji University), Ministry of Education, Shanghai, China
3. School & Hospital of Stomatology, Tongji University, Shanghai Engineering Research Center of Tooth Restoration and Regeneration, Shanghai 200072, China.

* These authors have equal contribution and are designated as co-first authors.

✉ Corresponding author: Liming Cheng, Department of Spine Surgery, Tongji Hospital, Tongji University School of Medicine, Shanghai 200065, China. E-mail: limingcheng@tongji.edu.cn.

Received: 2018.10.01; Accepted: 2018.11.28; Published: 2019.01.01

Abstract

Endoplasmic reticulum (ER) stress-induced neuronal apoptosis is a crucial pathological process of spinal cord injury (SCI). In our previous study, icariin (ICA) showed neuroprotective effects in SCI. However, the relationships between ER stress and ICA in SCI are unclear yet. Therefore, whether ICA could ameliorate SCI via attenuating ER stress was investigated *in vitro* and *in vivo*. Adult mice were established SCI model and received vehicle solution or ICA by gavage once per day *in vivo*. The primary cultured cells were treated with or without thapsigargin (TG), ICA or LY294002 to induce ER stress *in vitro*. Motor dysfunction, neuronal apoptosis, tissue damage and inhibition of PI3K/AKT pathway were induced by ER stress after SCI. But ICA administration significantly enhanced motor recovery and protected spinal cord tissues against infraction and hemorrhage, etc. post injury. Meanwhile, the expression of ER stress markers ATF6, IRE1α, GRP78, XBP1 and eIF2α was decreased, while the level of p-AKT/AKT was increased by ICA. Furthermore, ICA significantly inhibited the expression of ER stress apoptotic proteins caspase-12, CHOP, Bax/Bcl-2, caspase-9 and caspase-3. Moreover, immunofluorescence double staining indicated that ICA reduced GRP78, CHOP and TUNEL positive neurons following SCI. However, this beneficial effect of ICA was abolished by PI3K/AKT inhibitor LY294002 *in vitro*. Finally, ICA preserved the ultra-structure of ER by transmission electron microscope histologically. This study suggested that the neuroprotective effect of ICA on motor recovery and neuronal survival was related to attenuating ER stress via PI3K/AKT signaling pathway after SCI.

Key words: icariin, endoplasmic reticulum stress, spinal cord injury, neuroprotection, PI3K/AKT

Introduction

Spinal cord injury (SCI) is a fatal event with high morbidity and severe complications. Effective treatments are lacking due to complex molecular cascades affecting cell survival and neurological integrity which are not fully understood. The pathophysiology process of SCI includes the primary and the secondary injury. Primary injury is usually an irreversibly mechanical damage on spinal cord tissues immediately, while the secondary one leads to dynamic and complex patterns of biochemical and pathophysiological destructive, greatly worsening the damage caused by primary injury [1]. And it has been demonstrated that neuronal apoptosis has a crucial effect in this stage by inducing partial loss of behavioral and sensory function that expands through the spinal cord. Therefore, it is crucial to explore the specific molecular pathway mediating apoptosis in order to design an effective therapy for SCI.

In addition to the apoptosis induced by mitochondrial and death receptor signaling pathway, recent studies have indicated that neuronal apoptosis triggered by endoplasmic reticulum (ER) stress is vital in various diseases [2]. ER modulate proteins folding in eukaryotic cells, and ER stress could be caused by

various external factors including inflammation, oxidative stress and SCI. Unfolded protein response (UPR) is a reliable indicator of ER stress for enhancement of the ability of folding proteins and maintaining the cellular homeostasis, etc. The activating transcription factors 6 (ATF6), double-stranded RNA-activated protein kinase-like ER kinase (PERK) and inositol-requiring enzyme 1 (IRE1) are three critical markers associated with UPR [3]. Furthermore, the 78-kDa glucose regulation protein (GRP78), which is a Ca^{2+}-dependent molecular chaperones, is essential for UPR due to the binding with PERK, IRE1 and ATF6 under the normal physiological conditions. However, under the pathological conditions, GRP78 dissociates from these three proteins and actives them. The activated IRE1 and PERK can increase the level of the X-box-binding protein 1 (XBP-1) and the phosphorylation of α-subunit of eukaryotic translation initiation factor 2 (eIF2α), respectively. Although the UPR tends to maintain normal cellular function by removing misfolded proteins, the prolonged or excessive UPR eventually triggers apoptosis in SCI.

It has been demonstrated that apoptosis induced by ER stress is related to three pivotal pathways: the transcription of the CCAAT/enhancer-binding protein homologous protein (CHOP) [4], IRE1–tumor necrosis factor receptor-associated factor 2 (TRAF2) and caspase-12 [5]. CHOP activated by PERK and ATF6 could significantly inhibit the B cell lymphoma 2 (Bcl-2) gene, which is an important anti-apoptotic gene inhibiting Cytochrome C (Cyt C) release via mitochondrial outer membrane. TRAF2 recruited by IRE1 can activate caspase-12, and then the apoptosis executer caspase-9 and caspase-3. The previous study demonstrated that ER stress could cause apoptosis especially in neurons and oligodendrocytes [6]. Therefore, modulating UPR and inhibiting ER stress apoptotic pathway may present potential therapeutic strategies for SCI.

Icariin (ICA) is prenylated flavonol glycoside and the major active component isolated from the famous medical herb Epimedium. ICA has a wide range of efficacy, such as antioxidant effects, antibacterial effects and neuroprotection, etc [7-9]. For example, Pan et al. [8] suggested that ICA possessed antidepressant activities in Wistar rats with chronic mild stress. Furthermore, ICA could attenuate middle cerebral artery occlusion injury in rats [10]. Besides, Yang et al. [11] indicated that the composite scaffolds with ICA significantly promoted autologous nerve transplants and neuronal regeneration. However, the mechanism of neuroprotection of ICA in various CNS diseases is still controversial. Recent study suggested that ICA could decrease reactive oxygen species (ROS), CHOP and GRP78 to inhibit apoptosis mediated by ER stress in rat cardiac H9c2 cells [12]. Li et al. [13] also demonstrated that ICA protected ER and inhibited associated apoptosis of PC12 cell by directly degrading misfolded proteins. Therefore, according to our pre-experiment, we studied the potential role of ER in the effect of ICA on SCI.

Materials and Methods

Animals and Experimental Design

Experimental Animal Center of Tongji University (Shanghai, China) provided the 6–8 weeks old C57BL/6 male mice. The experiment was approved by the Ethical Committee of Tongji Hospital. The mice were assigned into three groups (randomization table assay): sham group (only T9–10 laminectomy and received a vehicle solution (0.9 % normal saline with 0.1 % DMSO) by gavage once per day), SCI group (established SCI model and received the vehicle solution in the same way) and ICA group (established SCI model and received ICA (Aladdin, Shanghai, China) at the dose of 50 μmol/kg). The volume of vehicle solution was the same with ICA in the study. More importantly, the appropriate dose of ICA was investigated and selected according to the previous study that the high dose of ICA had the better effect on the treatment of SCI [14-16].

Mice Model of SCI

The mice model of SCI was established by Precision Systems and Instrumentation Infinite Horizon (IH) Spinal Cord Impactor (NJ, USA) as described previously [17]. A laminectomy and moderate contusion injuries were performed at T9–10 without injuring the dura. The force and the dwell time were respectively 60 k dynes and 0 s. The success and consistency of SCI model were based on wagging of tail, fluttering and flaccid paralysis of hindlimbs and the data of the model.

Behavioral assessment

The motor function of hindlimbs in mice was evaluated at 0, 1, 2, 3, 4, 6 and 8 w following SCI according to the Basso Mouse Scale (BMS) scoring [18]. Mice were firstly exposed in a molded open field for 20 min/day for three days. The scales of the field are respectively 50 × 50 × 30 cm in long, wide, and high. The behavioral assessment was performed at the same time (16:00 p.m.) to maintain the repeatability and consistency of evaluation. And independent observation blinded to the experiment groups was performed twice.

Tissue preparation

For western blot, the mice were sacrificed under

anesthetized and perfused with normal saline solution transcardially to eliminate the blood at 1, 3, 7 d after SCI. The spinal cord tissues around the epicenter (± 0.5 cm) were dissociated, centrifugated and then detected by protein assay kit (BCA, Beyotime, Jiangsu, China).

For histological assessment and immunofluorescence staining, the mice were sequentially perfused with 0.9% normal saline and 4 % paraformaldehyde (in 0.1 M PBS, pH 7.4) transcardially under anesthetic. After fixed with 4 % paraformaldehyde overnight, the perilesional zones (epicenter ± 0.5 cm) were successively dehydrated with 20 % and then 30 % sucrose solution (with 0.1 M PBS) respectively for 24 h at 4 °C. Thereafter, the tissue was embedded in OCT compound (Sakura Finetechnical, Tokyo, Japan) to slice 5-μm transverse slices at -20 °C in a cryostat microtome (Leica, Germany). For each sample in different groups, six 5-μm sections were sequential selected at 200-μm intervals.

Histological assessment

HE staining kit and Nissl staining kit (Beyotime, Jiangsu, China) were applied to stain the slices according to the instructions. The extent of tissue damage was evaluated by observing the morphometric changes using an Olympus light microscope and a CCD camera (Leica DMI4000B, Germany). Furthermore, the number of survived neurons and the lesion size were quantitatively analyzed. All the procedures were performed in a blinded fashion.

Western blot assay

10 or 12 % sodium dodecyl sulfate polyacrylamide gel electrophoresis (SDS-PAGE) was carried out to separate the proteins. Afterwards, western transfer was performed with polyvinylidene fluoride (PVDF) membranes (Millipore, Bedford, MA, USA). After blocking, the membranes were incubated with each primary antibody (1:1000; CST or Abcam, USA) overnight. Afterwards, the corresponding secondary antibodies (1:2000; Abcam, USA) were incubated for 2 h. Then the proteins bands were visualized using enhanced chemiluminescence substrate (Millipore, Billerica, MA, USA) and photographed with Image Quant LAS 4000 (GE, USA). The grayscale value of interest proteins was analyzed by Image J software (NIH, Bethesda, MD, USA).

Immunofluorescence staining

After permeabilization and blocking for 1 h by PBS contained 5 % normal goat serum (Jackson ImmunoResearch, PA, USA) and 0.1 % Triton X-100, each primary antibody (1:500; CST or Abcam, USA) was applied to incubating sections overnight at 4°C. Meanwhile, species specific nonimmune Immunoglobulin G (IgG) was used to establish the negative control. Then the samples were incubated with Alexa Fluor® 488 goat anti-rabbit IgG (H + L) and Alexa Fluor® 594 goat anti-mouse IgG (H + L) (1:250, Life Technologies Corporation, USA) secondary antibody in the dark for 1-2 h. With respect to TUNEL staining, TUNEL mixture was used to stain at 37°C for 1 h (Roche, USA) and then 4', 6-Diamidino-2-Phenylindole (DAPI, 1:2000; Sigma Aldrich, St Louis, MO, USA) was selected to stain the nuclei for 2-3 min. Finally, confocal images were obtained using confocal laser scanning microscope (CLSM 800, Zeiss, Germany). Six randomly chosen fields within each section were observed to count the number of GRP78, AKT, CHOP or TUNEL positive neurons and quantitative analysis was performed.

Primary culture of spinal cord neurons

The spinal cord tissues were carefully moved into the 15 ml centrifuge tubes full of HBSS (Hanks Balanced Salt Solutions, Gibco, CA, USA) with Ca^{2+}, Mg^{2+} and 2 mg/ml papain (Sigma, USA), and then were cut into approximately 1 mm^3 pieces. After centrifugation, the supernatants were gently blown several times with a pipette and centrifuged again under the same conditions. Cell pellet was left and resuspended with the fresh Neurobasal medium (Gibco, CA, USA), then filtered through 40 μm cell strainer into 50 ml collection tubes. After centrifugeation, 2 mM glutamine (Gibco, CA, USA) and 2 % B-27 supplement (Gibco, CA, USA) were added into the medium to resuspend the remained cell-debris pellet again. A density of 1×10^6 live cells/ml were diluted and incubated at 37 °C overnight. Fresh neurobasal medium was used to replace half of the medium every another day until the seventh day.

Cell viability assay

Various concentrations of TG and ICA were selected to treat the cells with or without PI3K/AKT inhibitor LY294002 in the 96-well plate. At 37 °C, the cells were cultured for 4 h with 10 μl MTT reagent (Beyotime, Shanghai, China) at 5 % CO_2 in dark. Then, 100 μl DMSO was added to dissolve the formazan in each well. The measurement of optical density (OD) was perfomed by a microplate reader (Bio-Tek, USA) at 490 nm. The OD of treated group/ the OD of control group × 100 % was calculated as cell viability.

Transmission electron microscope (TEM)

The tissues were postfixed in 2.5% glutaraldehyde at 4 °C overnight. Then the spinal cord dorsal horn (epicenter ± 2 mm) was cut into approximate 1 mm^3 pieces. The samples were then blocked by 1% osmium tetroxide in 0.1 M cacodylate buffer for 2 h (pH7.2). Afterwards, the tissues were dehydrated in

gradient alcohol solutions and 100% acetone, and then embedded in Epon 812 using standard procedures. At last, lead citrate and uranyl acetate were used to stain the tissues which were sliced into ultrathin sections with 50-60 nm thickness. A TEM (JEM-1230, Japan Electron Optics Laboratory Co. Ltd., Japan) was applied to observe.

Statistical Analysis

All results were expressed as mean ± standard deviation (SD) (n=6). Statistical differences were analyzed with one-way analysis-of-variance (ANOVA) and the SNK test (SPSS 16.0, USA). $P < 0.05$ means statistically significant.

Results

ER stress and neuronal apoptosis were induced in the mice model of SCI

At 1, 3 and 7 d post injury, results showed that the expression of ATF6, IRE1α, GRP78, XBP-1 and eIF2α increased dramatically in SCI group (Figure 1A, B). Furthermore, confocal images revealed that there were nearly no apoptotic neurons in the sham group (Figure 1B, C). But the positive neurons were observed in the SCI group during the process of injury. Moreover, the highest number of TUNEL positive neurons could be found at 3 d post operation. Besides, the expression of CHOP and caspase-12 also significantly increased and reached the peak at 3 d after SCI. Consistent with our previous research, the following studies were investigated at 3 d after SCI [19].

ICA promoted motor recovery and ameliorated tissue damage in SCI

The mice of SCI group exhibited dramatically decrease in BMS score. In ICA group, BMS score was not statistically different from that of SCI group at 1 w. However, the continuous treatment of ICA enhanced motor recovery according to the evaluation compared with the SCI group at 2, 3, 4, 6 and 8 w after SCI.

Furthermore, Figure 2C showed that the tissues of SCI group showed marked structural damage compared with the sham group histopathologically. In comparison, the treatment of ICA dramatically attenuated the destruction. The extent of focal hemorrhage, infraction and cavity in the gray matters of ICA group was mild and in between that of the sham group and SCI group. And there were less karyopyknosis, necrosis and reactive glial cells in the tissues of ICA group which exhibited more clear boundaries (Scale bars = 100 μm). Moreover, the Nissl staining showed that the survived neurons decreased remarkably, while the lesion size increased significantly in the SCI group (Figure 2E, F). However, Nissl staining of the ICA group revealed more Nissl bodies but less karyopyknosis and cavities. It demonstrated that there were a larger numbers of survived neurons but smaller area of lesion size in the ICA group.

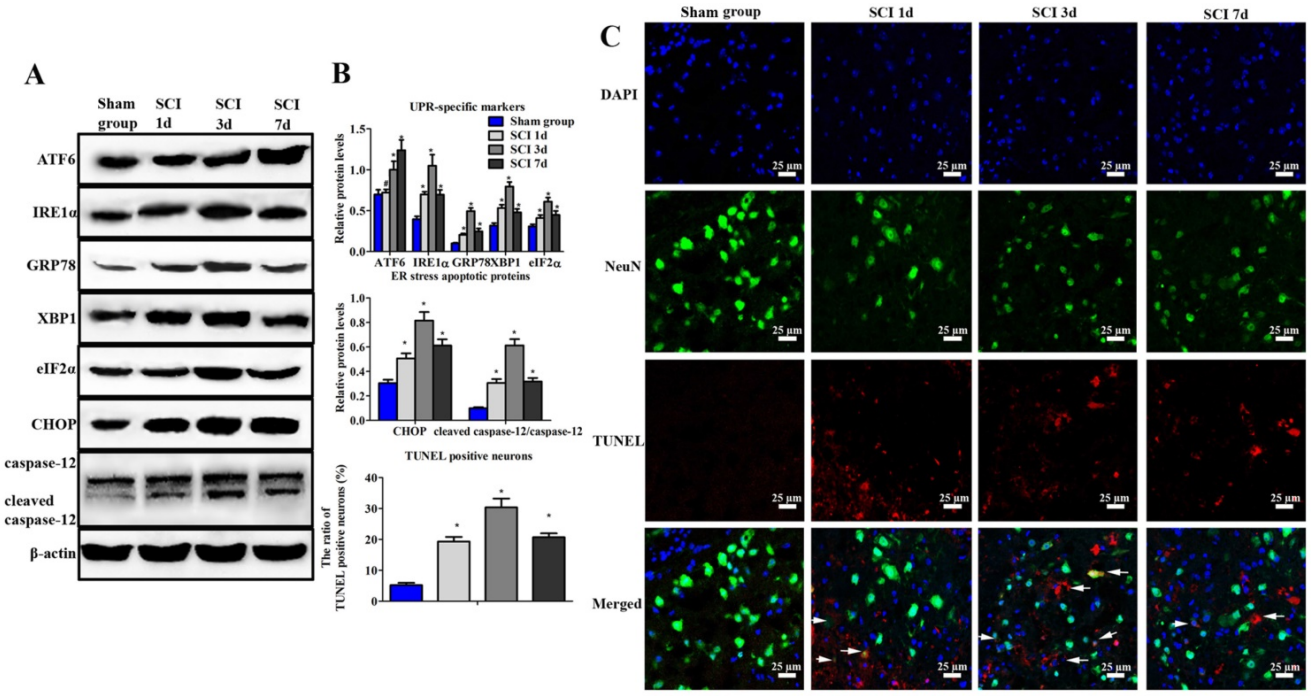

Figure 1. Evaluation of ER stress and neuronal apoptosis induced by SCI. (A) Western blot assay of UPR-specific proteins and ER stress apoptotic protein. (B) The quantitative analysis. (C) immunofluorescence staining of TUNEL positive neurons (Scale bars = 25 μm). ER stress and neuronal apoptosis were induced by SCI at 1, 3, 7 d post injury. $^{*}P < 0.01$, $^{\#}P < 0.05$ compared with SCI group.

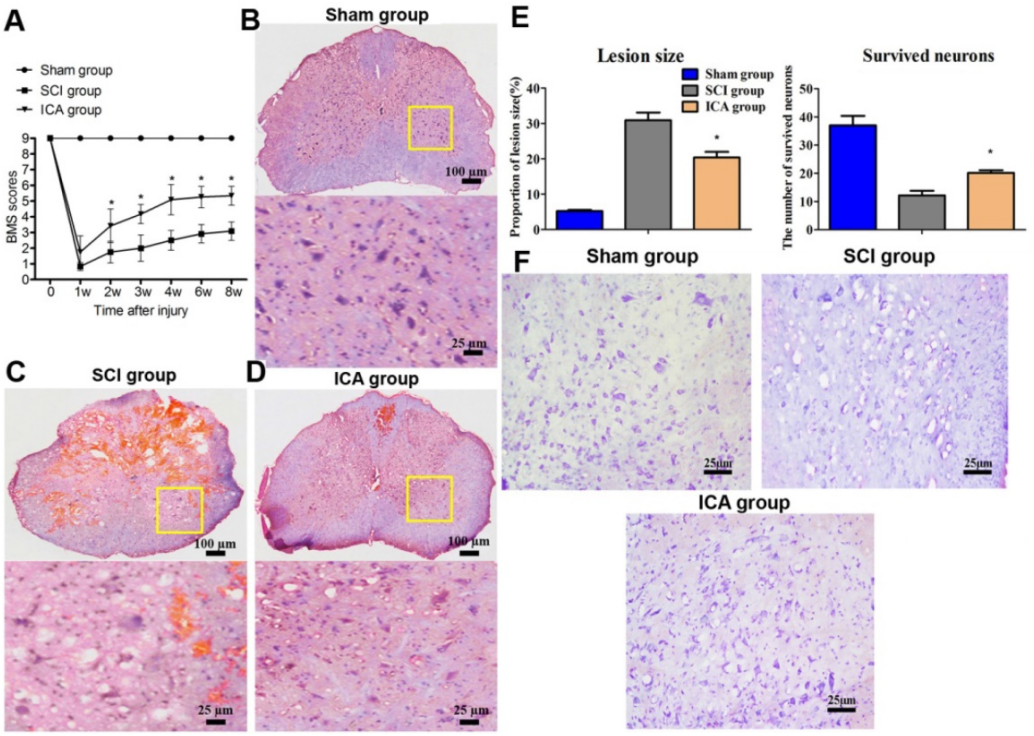

Figure 2. Evaluation of tissue damage and motor function in SCI. (A) BMS scores. (B-D) HE staining (Scale bars = 100 μm). (E) Quantitative analysis of lesion size and survived neurons. (F) Nissl staining (Scale bars = 25 μm). ICA significantly promoted motor recovery at 2, 3, 4, 6, 8 w. ICA significantly increased the number of survived neurons and decreased the area of lesion size of tissues. *$P < 0.05$ compared with SCI group.

ICA attenuated ER stress and activated PI3K/AKT pathway in SCI

Comparing with SCI group, the level of UPR markers was dramatically decreased by ICA administration at 3 d after injury (Figure 3A & D). Furthermore, Figure 3B showed that the number of GRP78$^+$ neurons of SCI group increased greatly at 3 d post injury. But ICA significantly decreased the number of GRP78 positive neurons. Furthermore, the relative level of p-AKT/AKT and AKT positive neurons were decreased in SCI group which implied the down-regulated of PI3K/AKT pathway induced by SCI (Figure 3F). After ICA administration, it was found that the level of p-AKT/AKT and the number of AKT$^+$ neurons were increased significantly (Figure 3C, F & G). In order to further investigate the potential role of PI3K/AKT pathway in the relationship between ICA and SCI, the inhibitor of PI3K/AKT pathway LY294002 was used in the following studies *in vitro*.

ICA inhibited neuronal apoptosis induced by ER stress in SCI

In the SCI group, the level of CHOP, cleaved caspase-9/caspase-9, Bax/Bcl-2, cleaved caspase-12/caspase-12 and cleaved caspase-3/caspase-3 all increased significantly at 3 d post injury which indicated the activation of ER stress-induced apoptosis (Figure 4A). However, the expression of these apoptotic proteins was dramatically decreased by ICA. Furthermore, immunofluorescence staining also showed that ICA treatment significantly decreased the number of CHOP$^+$ and TUNEL$^+$ neurons (Figure 4B-C).

The inhibition of ER stress-induced neuronal apoptosis by ICA is associated with PI3K/AKT pathway

In the present study, we observed the development of neurons derived from mature spinal cord through an Olympus light microscope. The dispersed cells exhibited a translucent and circle shape with uniform cytoplasm and surrounding halo after initial inoculation (Figure 5A). At 1 d, almost half of cells prolonged short protrusions, while dead cells and debris suspended in NDM. After culturing for 5 d, neuron bodies gradually became hypertrophic and plump on the shape of triangle, cambiform or ellipse, etc. At 7 d, it was obvious that neuron bodies were clearly visible, large and full with three-dimensional appearance and network connections between neurons. Furthermore, the ratio of cells double labeled by DAPI and β-III Tubulin was up to 80% of the total cell volume according to the results of immunofluorescence staining (Figure 5C). This result ensured that primary cultured spinal cord neurons with high purity distinguished from other types of glial cells were available for the following research *in vitro*.

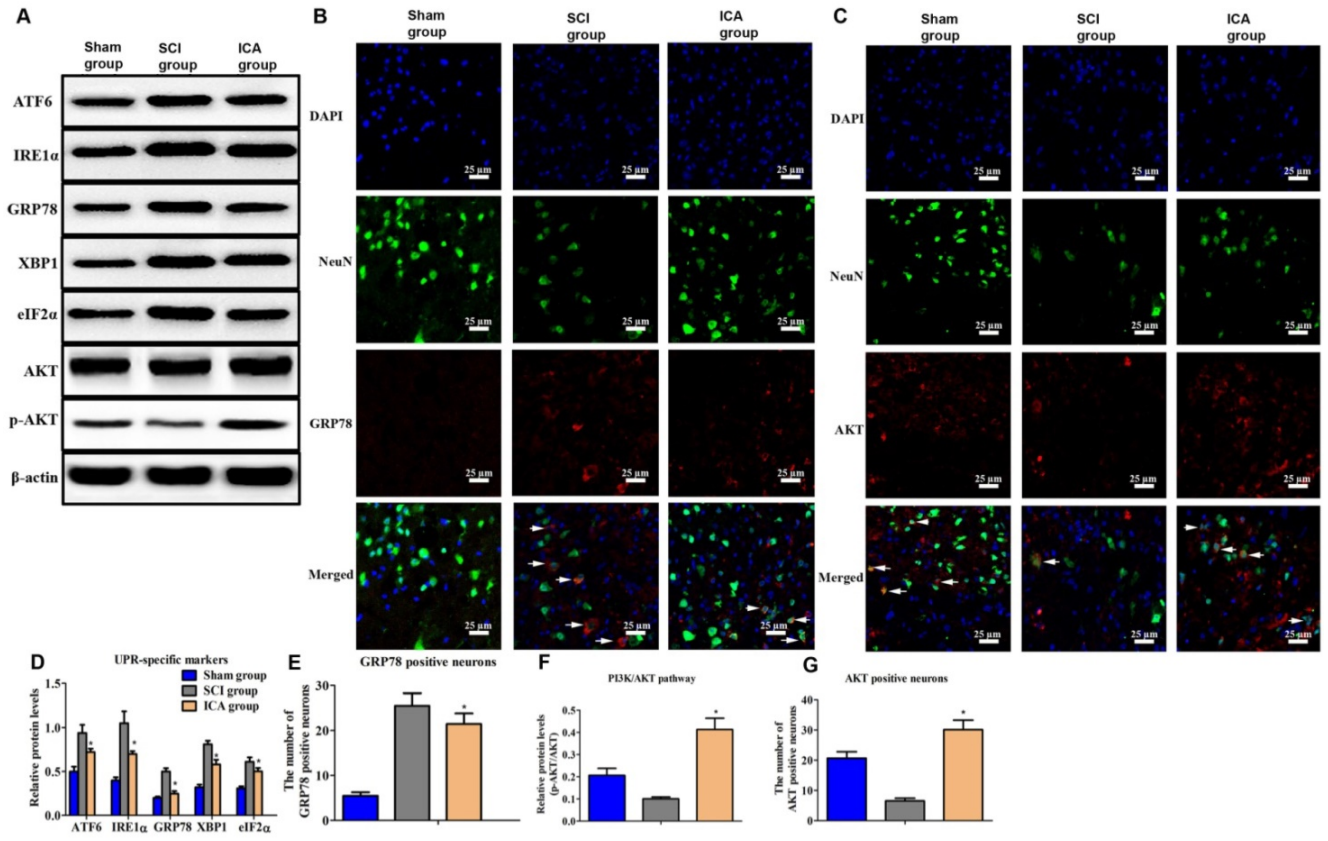

Figure 3. Investigation the effect of ICA on ER stress and PI3K/AKT pathway in SCI. (A, B, C) Western blot and immunofluorescence staining assays of UPR specific proteins and AKT (Scale bars = 25 μm). (D-G) The quantitative analysis. ICA significantly attenuated ER stress and activated PI3K/AKT pathway after SCI. *$P < 0.05$ compared with SCI group.

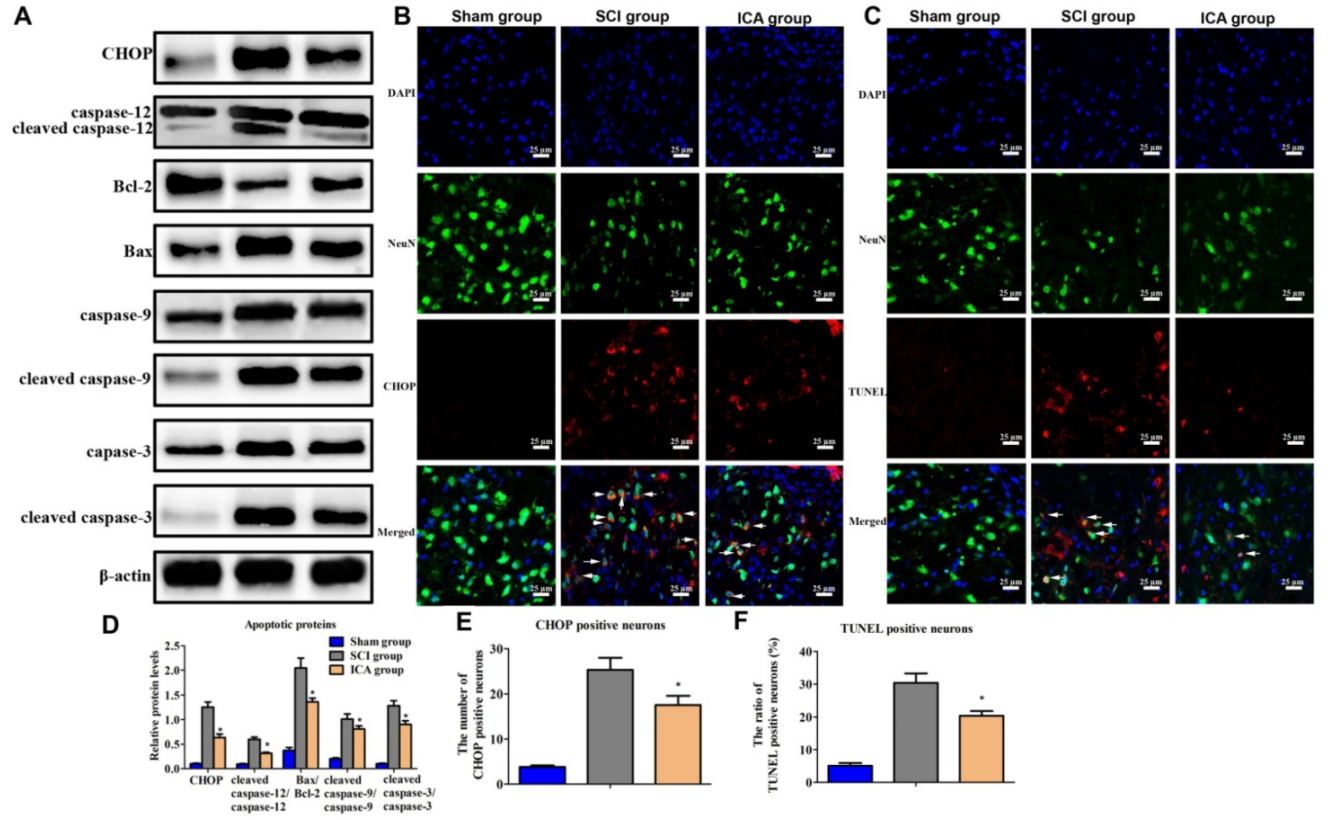

Figure 4. Investigation the effect of ICA on ER stress apoptotic pathway in SCI. (A) Western blot assays of proteins of ER stress apoptotic pathway. (C, D) Immunofluorescence staining of CHOP or TUNEL positive neurons (Scale bars= 25 μm). (D-E) The quantitative analysis. ICA significantly inhibited ER stress apoptotic pathway after SCI. *$P < 0.05$ compared with SCI group.

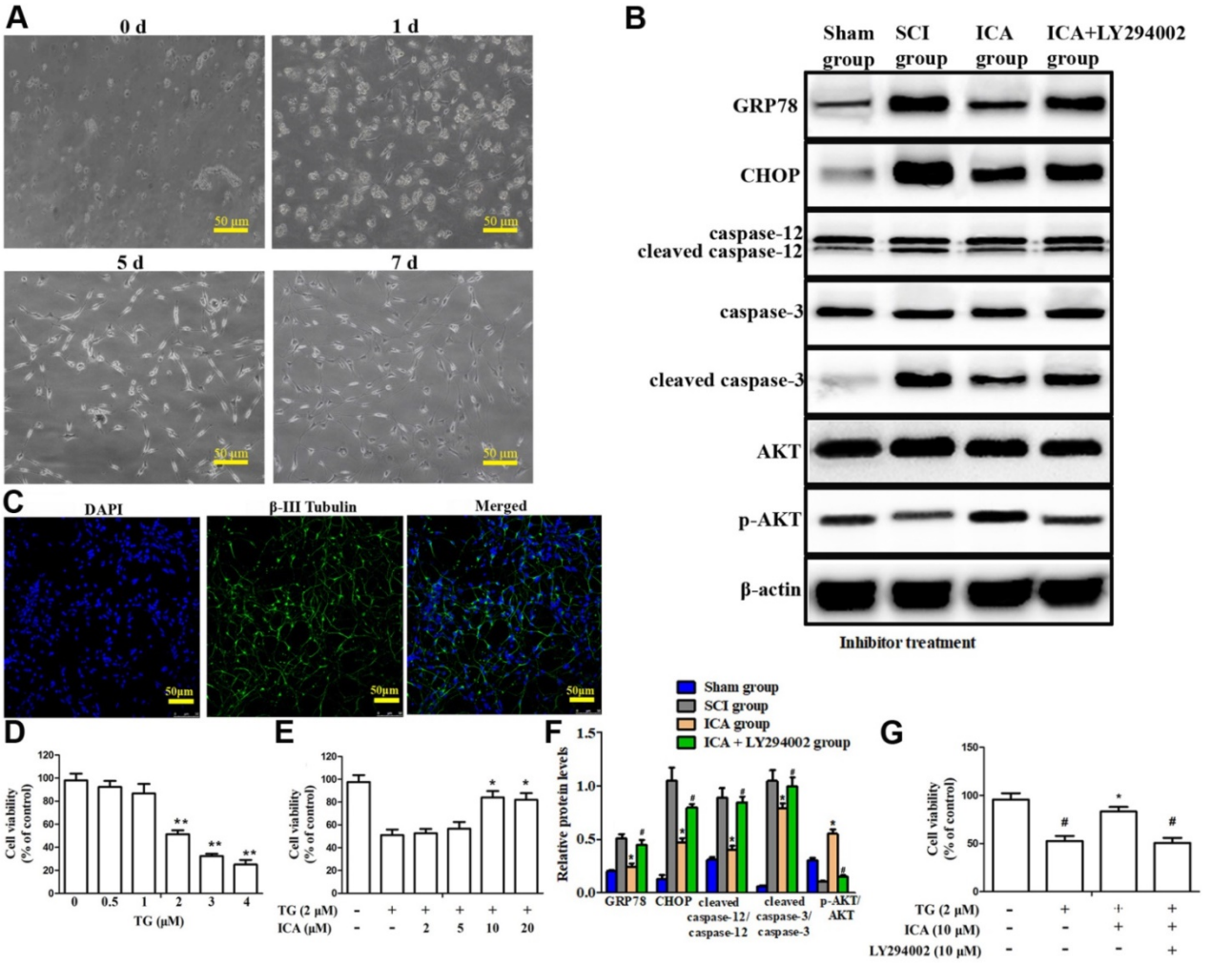

Figure 5. Investigation the PI3K/AKT signaling pathway in the anti-apoptotic effect of ICA *in vitro*. (A) Observation of cell morphology (Scale bars = 50 μm). (B) Western blot assays of ER stress-induced apoptosis. (C) Immunofluorescence staining (Scale bars = 50 μm). (D, E) Cell viability after the treatment with TG and with or without ICA. (F) Quantitative analysis of western blot assays. (G) Cell viability after treatment with or without TG, ICA and LY294002. The primary cultured spinal cord neurons were cultured with great growth state, appropriate density and high purity. The cell viability decreased by half at 2 μM TG. The cell viability was significantly increased by ICA pretreatment (10 - 20 μM). ICA decreased the expression of apoptotic proteins and enhanced cell viability after SCI. However, LY294002 administration significantly reversed this beneficial effect. $^{**}P < 0.05$ compared with control; $^{*}P < 0.05$ compared with TG or SCI group; $^{\#}P < 0.05$ compared with ICA group.

The doses of TG and ICA to be used were first determined based on cell viability assay. As shown in Figure 5D, following TG exposure (0.5 - 4 μM) for 12 h, the cell viability decreased by half at 2 μM TG compared with 0 μM. Nevertheless, this trend was dramatically attenuated by ICA pretreatment (10 - 20 μM) for 2 h prior to TG exposure. Therefore, 10 μM ICA was used in the following experiments. The results showed that the level of apoptotic proteins increased, while the expression of p-AKT/AKT decreased significantly in TG group. Nevertheless, the trend was reversed after ICA administration that the level of p-AKT/AKT increased, while the level of the apoptotic proteins decreased significantly (Figure 5B). Moreover, MTT results indicated that ICA significantly enhanced the cell viability after TG-induced ER stress *in vitro*. By contrast, these beneficial effects of ICA were evidently reversed when LY294002 was applied (Figure 5F-G).

ICA preserved the ultra-structure of ER in SCI and the schematic

As shown in Figure 6A, in the sham group, results showed that ER was regular with distinct rows and many ribosomes attached on membranes. However, the ultra-structure changed significantly at 3 d after SCI that exhibiting larger and vacuole-like shapes with many shedding ribosomes. And the ultra-structure of ER was not distinct after suffering from SCI. In contrast, ICA administration significantly ameliorated the destruction of ER structure. The ER in the ICA group was slightly larger in shapes compared with that in the sham group, and there were fewer shedding ribosomes than those in the SCI group. Moreover, the schematic shows the possible mechanisms related to ER in SCI.

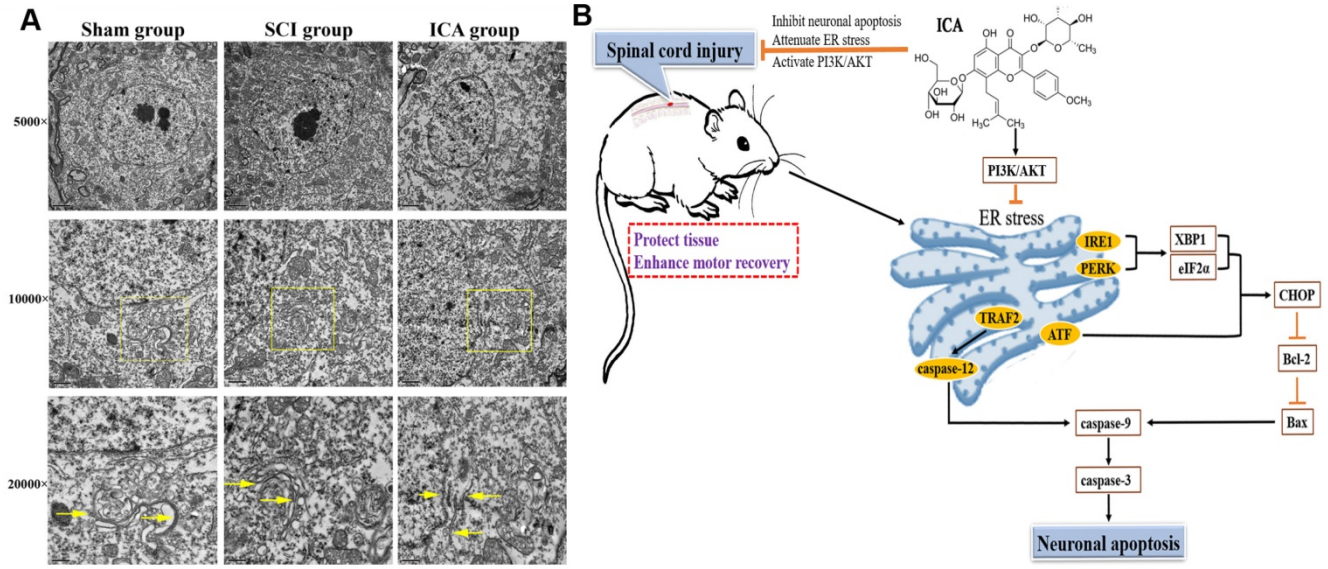

Figure 6. Evaluation the ultra-structure of ER and the schematic. (A) ICA treatment significantly preserved the ultra-structure of ER after SCI compared with the SCI group. Yellow arrows indicated the ultra-structure of ER. (Scale bars= 2 μm, 1 μm, 0.5 μm). (B) ICA attenuates ER stress and inhibits ER stress apoptotic pathway in the mice model of SCI by activating the PI3K/AKT signaling pathway.

Discussion

Recent studies of ICA on various nervous system diseases [20, 21] have aroused wide concern of the mechanisms of inhibiting neuronal apoptosis by ICA. The results of this study demonstrated that the neuroprotective effect of ICA on SCI was connected with attenuating ER stress via PI3K/AKT signaling pathway (Figure 6B). However, we cannot rule out the additional potential mechanisms due to the relationships between ER and other organelles or signaling pathways. In our previous study, the pivotal relationship between mitochondrial and SCI was investigated [19]. However, the crosstalk between ER and mitochondria remains unclear. Both mitochondria and ER are crucial organelles for normal function and survival of neurons and non-neuron cells. Banerjee et al. [22] found that mitochondrial dysfunction could be induced by ER stress *in vitro*. Moreover, our previous study indicated that exendin-4 could attenuate neuronal apoptosis by ameliorating mitochondria dysfunction after SCI [4, 23]. According to the present study, the possibly synchronous modulation of mitochondria and ER by ICA may be an underlying mechanism.

The precise signaling pathways that mediate ER stress in neuronal damage after SCI are not yet fully elucidated. And it also has been demonstrated that multiple effects are the pivotal characteristic of Chinese herb. Recent study illustrated the pivotal role of PI3K/AKT in the inhibition of apoptosis caused by ER stress in SCI [1]. PI3K/AKT pathway controls various cellular events, including proliferation, stress and apoptosis. Two of the crucial downstream proteins of PI3K/AKT are Bax and Bcl-2, which are related to apoptosis. Cheng et al. found that promotion of AKT phosphorylation could increase Bcl-2 expression, thus decreasing the levels of Bax and cleaved caspase-3 in SCI [24]. Moreover, PI3K/AKT pathway is also involved with autophagy [25]. Autophagy is a 'self-eating' pathway involved with inflammation and ER Stress after SCI [26, 27]. Studies showed that the administration of rapamycin could reduce neuronal apoptosis and locomotor impairment via promoting autophagy after SCI [25, 28]. Hence, the inhibitory effect of ICA on neuronal apoptosis may be involved with the modulation of autophagy and other mechanisms.

Although it is the first time to elucidate the relationships between ICA and ER in SCI, the analysis of difference in temporal and specific cellular activation in ER stress remains unclear. Ohri et al. found that UPR markers of neurons only appeared at 6 and 24 h post SCI, while lasted at least for 72 h in oligodendrocytes and astrocytes [17]. Penas et al. [6] indicated that mRNA of CHOP, GRP78 and XBP1 raised at 6 h and reached the top at 12 h post injury. But Zhang et al. [1] found that expression and location of CHOP, caspase-12 and GRP78 increased at 1 d after injury, reached the maximal at 3 d and decreased from 7 d after SCI. This is consistent with our results that most UPR markers and apoptotic proteins reached the peak at 3 d after SCI (Figure 1). The temporal difference among previous studies may be involved with different SCI models, diverse animals or multiple interventions.

In addition, even though our results revealed that inhibiting neuronal ER stress could promote behavioral function in SCI, the apoptosis of glial cells

also has pivotal role in CNS diseases [19, 23]. Glial cells are identified generally as astrocytes, oligodendrocytes, and microglia over the years. Oligodendrocytes could promote remyelination and functional recovery in SCI and demyelinating diseases [29, 30]. 20-40 % of all types of cells in CNS of the mammalian are consist of astrocytes that regulating the microenvironment [31]. Resident microglia are the main immune cells activating immunoreaction and inflammation in the process of SCI. With respect to ERS in SCI, Ohri et al. [17] found that most of astrocytes in spinal cord tissues recovered from ER stress, while oligodendrocytes are sensitive to ER stress and deletion of CHOP could lead to inhibiting oligodendrocyte loss and promoting hindlimb locomotion after SCI. Similarly, sodium valproate was confirmed to reduce the CHOP level, increase the relative number of oligodendrocytes and promote behavioral function after SCI [32]. Besides, the inhibition of astrogliosis and motor recovery after SCI was associated with the decrease of the astrocytes specific ER stress transducer [33]. However, astrocytic and microglial scars have also been regarded as barriers to the regeneration of transected axons across lesion tissues after SCI [34]. Hence, we speculated that the precise mechanisms associated with apoptosis and ER stress may be cell specific in SCI. And the extent of up or down-modulation of oligodendrocytes, astrocytes or microglia may become a new target in the treatment of SCI.

Our present study demonstrated that ICA administration inhibited neuronal apoptosis and improved the functional recovery in SCI through the activation of PI3K/AKT signaling pathway both *in vivo* and *vitro*. This indicated that therapies targeting on ER stress may be promising in the treatment of CNS disease.

Acknowledgements

This research was supported by Key projects of National Natural Science Foundation of China (No. 81330030); the National Key research and Development Program (No. 2016YFA0100800).

Competing Interests

The authors have declared that no competing interest exists.

References

1. Zhang HY, Zhang X, Wang ZG, Shi HX, Wu FZ, Lin BB, et al. Exogenous basic fibroblast growth factor inhibits ER stress-induced apoptosis and improves recovery from spinal cord injury. CNS Neuroscience & Therapeutics. 2013; 19: 20-9.
2. Rong F, Gao X, Liu K, Wu J. Methotrexate remediates spinal cord injury *in vivo* and *in vitro* via suppression of endoplasmic reticulum stress-induced apoptosis. Experimental & Therapeutic Medicine. 2018; 15:4191-8.
3. Zhang HY, Wang ZG, Lu XH, Kong XX, Wu FZ, Lin L, et al. Endoplasmic Reticulum Stress: Relevance and Therapeutics in Central Nervous System Diseases. Molecular Neurobiology. 2015; 51: 1343-52.
4. Wang J, Zhang M, Li H, Li G, Jia Z, Sun P, et al. Berberine improves motor function recovery by inhibiting endoplasmic reticulum stress-induced neuronal apoptosis via AMPK activation in rats with spinal cord injury. International Journal of Clinical & Experimental Pathology. 2017; 10: 4900-11.
5. Wan S, Shi P, Zhang X, Gu C, Fan S. Stronger expression of CHOP and caspase 12 in diabetic spinal cord injury rats. Neurological Research. 2014; 31: 1049-55.
6. Penas C, Guzmán MS, Verdú E, Forés J, Navarro X, Casas C. Spinal cord injury induces endoplasmic reticulum stress with different cell-type dependent response. Journal of Neurochemistry. 2007; 102: 1242-55.
7. Wang L, Zhang L, Chen ZB, Wu JY, Zhang X, Xu Y. Icariin enhances neuronal survival after oxygen and glucose deprivation by increasing SIRT1. European Journal of Pharmacology. 2009; 609: 40-4.
8. Pan Y, Wang FM, Qiang LQ, Zhang DM, Kong LD. Icariin attenuates chronic mild stress-induced dysregulation of the LHPA stress circuit in rats. Psychoneuroendocrinology. 2010; 35: 272-83.
9. Li ZJ, Yao C, Liu SF, Chen L, Xi YM, Zhang W, et al. Cytotoxic effect of icaritin and its mechanisms in inducing apoptosis in human burkitt lymphoma cell line. Biomed Research International. 2014; 2014: 391512.
10. Xiong D, Deng Y, Huang B, Yin C, Liu B, Shi J, et al. Icariin attenuates cerebral ischemia-reperfusion injury through inhibition of inflammatory response mediated by NF-κB, PPARα and PPARγ in rats. International Immunopharmacology. 2016; 30: 157-62.
11. Yang CR, Chen JD. Preparation and biological evaluation of chitosan-collagen-icariin composite scaffolds for neuronal regeneration. Neurological Sciences. 2013; 34: 941-7.
12. Zhang Q, Li H, Wang S, Liu M, Feng Y, Wang X. Icariin Protects Rat Cardiac H9c2 Cells from Apoptosis by Inhibiting Endoplasmic Reticulum Stress. International Journal of Molecular Sciences. 2013; 14: 17845-60.
13. Li F, Gao B, Dong H, Shi J, Fang D. Icariin induces synoviolin expression through NFE2L1 to protect neurons from ER stress-induced apoptosis. Plos One. 2015; 10: e0119955.
14. Tohda C, Nagata A. Epimedium koreanum Extract and Its Constituent Icariin Improve Motor Dysfunction in Spinal Cord Injury. Evidence-Based Complementray and Alternative Medicine. 2012; 2012: 731208.
15. Guo J, Li FQ, Gong Q, Lu Y, Shi J. Protective effects of icariin on brain dysfunction induced by lipopolysaccharide in rats. Phytomedicine. 2010; 17: 950-5.
16. Zhu HR, Wang ZY, Zhu XL, Wu XX, Li EG, Xu Y. Icariin protects against brain injury by enhancing SIRT1-dependent PGC-1alpha expression in experimental stroke. Neuropharmacology. 2010; 59: 70-6.
17. Ohri SS, Maddie MA, Zhao Y, Qiu MS, Hetman M, Whittemore SR. Attenuating the endoplasmic reticulum stress response improves functional recovery after spinal cord injury. Glia. 2011; 59: 1489–502.
18. Basso DM, Fisher LC, Anderson AJ, Jakeman LB, Mctigue DM, Popovich PG. Basso Mouse Scale for locomotion detects differences in recovery after spinal cord injury in five common mouse strains. Journal of Neurotrauma. 2006; 23: 635.
19. Li HT, Zhao XZ, Zhang XR, Li G, Jia ZQ, Sun P, et al. Exendin-4 Enhances Motor Function Recovery via Promotion of Autophagy and Inhibition of Neuronal Apoptosis After Spinal Cord Injury in Rats. Molecular Neurobiology. 2016; 53: 4073-82.
20. Liu B, Zhang H, Xu C, Yang G, Tao J, Huang J, et al. Neuroprotective effects of icariin on corticosterone-induced apoptosis in primary cultured rat hippocampal neurons. Brain Research. 2011; 1375: 59-67.
21. Zeng KW, Ko H, Yang HO, Wang XM. Icariin attenuates β-amyloid-induced neurotoxicity by inhibition of tau protein hyperphosphorylation in PC12 cells. Neuropharmacology. 2010; 59: 542-50.
22. Banerjee K, Keasey MP, Razskazovskiy V, Visavadiya NP, Jia C, Hagg T. Reduced FAK-STAT3 signaling contributes to ER stress-induced mitochondrial dysfunction and death in endothelial cells. Cellular Signalling. 2017; 36: 154-62.
23. Li H, Jia Z, Li G, Zhao X, Sun P, Wang J, et al. Neuroprotective effects of exendin-4 in rat model of spinal cord injury via inhibiting mitochondrial apoptotic pathway. International Journal of Clinical & Experimental Pathology. 2015; 8: 4837-43.
24. Cheng Q, Meng J, Wang XS, Kang WB, Tian Z, Zhang K, et al. G-1 exerts neuroprotective effects through G protein-coupled estrogen receptor 1 following spinal cord injury in mice. Bioscience Reports. 2016; 36: e00373.
25. Sekiguchi A, Kanno H, Ozawa H, Yamaya S, Itoi E. Rapamycin promotes autophagy and reduces neural tissue damage and locomotor impairment after spinal cord injury in mice. Journal of Neurotrauma. 2012; 29: 946-56.
26. Wu F, Wei X, Wu Y, Kong X, Hu A, Tong S, et al. Chloroquine promotes the recovery of acute spinal cord injury by inhibiting autophagy-associated inflammation and endoplasmic reticulum stress. Journal of Neurotrauma. 2018; 35: 1329-44.
27. Yang F, Liao J, Pei R, Yu W, Han Q, Li Y, et al. Autophagy Attenuates Copper-induced Mitochondrial Dysfunction by Regulating Oxidative Stress in Chicken Hepatocytes. Chemosphere. 2018; 204: 36-43.
28. Wang ZY, Liu WG, Muharram A, Wu ZY, Lin JH. Neuroprotective effects of autophagy induced by rapamycin in rat acute spinal cord injury model. Neuroimmunomodulation. 2014; 21: 257-67.

29. Wang HF, Liu XK, Li R, Zhang P, Chu Z, Wang CL, et al. Effect of glial cells on remyelination after spinal cord injury. Neural Regeneration Research . 2017; 12: 1724-32.
30. Lin Y, Huang G, Jamison S, Li J, Harding HP, Ron D, et al. PERK activation preserves the viability and function of remyelinating oligodendrocytes in immune-mediated demyelinating diseases. American Journal of Pathology. 2014; 184: 507-19.
31. Herculano-Houzel S. The glia/neuron ratio: how it varies uniformly across brain structures and species and what that means for brain physiology and evolution. Glia. 2014; 62: 1377-91.
32. Lee JY, Maeng S, Kang SR, Choi HY, Oh TH, Ju BG, et al. Valproic Acid Protects Motor Neuron Death by Inhibiting Oxidative Stress and Endoplasmic Reticulum Stress-Mediated Cytochrome C Release after Spinal Cord Injury. Journal of Neurotrauma. 2014; 31: 582-94.
33. Takazawa A, Kamei N, Adachi N, Ochi M. Endoplasmic reticulum stress transducer old astrocyte specifically induced substance contributes to astrogliosis after spinal cord injury. Neural Regeneration Research. 2018; 13: 536-40.
34. Anderson MA, Burda JE, Ren Y, Ao Y, O'Shea TM, Kawaguchi R, et al. Astrocyte scar formation aids central nervous system axon regeneration. Nature. 2016; 532: 195-200.